Assessment of Power Harvesting in Electronic Modules Using Phase Change Material with Null Electricity: An Experimental Study

K Gopi Kannan*, R Kamatchi*‡

*School of Mechanical Engineering, Vellore Institute of Technology, Vellore – 632 014, India.

(gopimetier@gmail.com, rkkamatchi@gmail.com)

‡ Corresponding Author; R Kamatchi, School of Mechanical Engineering, Vellore Institute of Technology, Vellore – 632 014, India, Tel: +91 9944405215, rkkamatchi@gmail.com

Received: 23.10.2020 Accepted:25.11.2020

Abstract- In this work, the assessment of power harvesting in electronic modules during its operation is experimentally investigated. The phase change material (PCM) based natural cooling is analyzed with a developed model using different circulating fluids such as DI water, ethanol, and methyl acetate respectively. The experiments are conducted to evaluate the power harvesting by PCM for circulating fluids at the different heat input between 60 and 110 W. The highest percentage of waste heat extraction obtains for methyl acetate of about 98.7% whereas 96.5% and 97.7% for DI water and ethanol respectively. It is because of the low boiling point and heat of evaporation at high heat input. The thermal resistance of methyl acetate is less of about 0.237 K/W while 0.655 and 0.398 K/W for DI water and ethanol respectively owing to high vapor flow rate and less subcooling effect. The maximum power harvested by PCM with the effect of vapourized methyl acetate is found as 9.41 W owing to less time to reach the steady-state temperature (SST) of PCM at 110 W.

Keywords Circulating fluids, waste heat, electronic modules, PCM, power harvesting.

1. Introduction

In recent decades, conversion of waste heat to useful power and energy-saving are the hefty task to scientists and researchers [1-5]. Also, power consumption is increased by 2% per year all over the world. To mitigate this problem, recovery of waste heat with different techniques is experimentally investigated by many authors [6,7]. However, latent heat storage using phase change material provides high energy storage stability and compactness [8]. Also, thermosyphon aid PCM storage would be of higher heat extraction rate as compared with thermal enhancers such as foam, fins and nanoparticles.

PCMs are the potential medium to store and release the latent heat energy while it undergoes a phase change [9,10]. Baby et al. [11] experimented on the heat transfer performance of PCM based aluminium heat sink. The two different kinds of PCMs such as n-eicosane and paraffin are used. They concluded that the paraffin-based heat sink is found to be an optimum one due to high power density. The PCM integrated thermal management unit for a compact electronic component is studied by Alawadhi et al. [12]. The results indicated that reliable operation can be obtained to avoid overheats and thermally induced fatigue using PCM in the heat sink. Sahoo et al. [13] reported the emerging trends of thermal conductivity enhancers (TCE) based on the heat sink for electronic cooling. The TCE filled metallic PCM is desirable for various thermal performance parameters. Nevertheless, the high density of metallic PCM is unsuited for less weight design of the heat sink.

Thermosyphon is a widely used gravity assist technique. The circulating fluids are used to remove heat flux from an electronic device without the use of any external aid. In general, it consists of three sections viz. evaporation, adiabatic, and condensation. The circulating liquid fluid converts the phase from liquid to vapour in the evaporation region. Then, it rises to the adiabatic section due to density variation where it releases the heat of evaporation. The condensed liquid comes back into the evaporative section through capillary action [14,15]. Samba et al. [16] developed a thermosyphon loop model for cooling the outdoor telecommunication device. They revealed that the thermosyphon cooling is twice better than air forced convective cooling owing to the absence of a high power supply. Liu et al. [17] experimentally studied the on-board ship electronic cooling system using closed-loop thermosyphon with water charged unit. The result showed that thermal performance is higher at maximum heat load by low thermal resistance and the heat removal is attained until 145 W/cm^2. Zhang et al. [18] reported the thermosyphon is an effective heat transfer unit, where the rate of heat removal is increased by boiling heat transfer and grooved evaporation region.

Heat transfer enhancement by thermosyphon used nanofluids is investigated by Kamyar et al. [19]. They identified that the performance is increased by the increase of heat transfer coefficient and a decrease in thermal resistance by 65%. The flat thermosyphon method is used in a heat spreader for electronic cooling. The results showed that the heat removal ability is obtained up to 10 W/cm^2 for the thermal resistance of about 0.07 K/W [20]. The different parameters of working fluids are investigated by Palm et al. [21] for a two-phase thermosyphon system used in electronic cooling. It is concluded that lower temperature difference can be achieved by an increase of pressure level. Also, there is no ideal heat transfer fluid for cooling the electronic device. Li et al. [22] studied the pool boiling thermosyphon unit for cooling the light-emitting diodes. DI water is used as a heat transfer fluid. The result indicated that maximum heat flux up to 60W/cm^2. Krishna et al. [23] investigated the thermal performance of a heat pipe with PCM for electronic cooling. Tricosane with Al_2O_3 is used as PCM for energy storage around the adiabatic section of the heat pipe. The result presented the evaporator temperature of the heat pipe is decreased by 25.75% which causes 53% power can be saved by Ne-PCM compared to a traditional heat pipe.

The objective of the present work is not only to extract the waste heat from electronic modules but also to store the energy in PCM for future use. In the present study, the thermosyphon aid PCM storage is investigated to dissipate the waste heat from electronic modules without the use of electrical power. The enhanced thermal performance viz. the percentage of waste heat extraction and thermal resistance for DI water, ethanol and methyl acetate are studied and compared. Also, the temperature variation and power saving by PCM using various circulating fluids are analyzed for influencing heat inputs.

2. Experimental

2.1. Materials

In this study, the various circulating fluids such as DI water, ethanol and methyl acetate are used and the thermophysical properties are listed in Table 1. Paraffin wax (RT 53) is taken as PCM to absorb latent heat from circulating fluids owing to better stability after several repeated cycles [24]. The properties of paraffin wax are presented in Table 2. Also, the thermogravimetric (TGA) analysis is done by the range from 20 °C and 440 °C at the

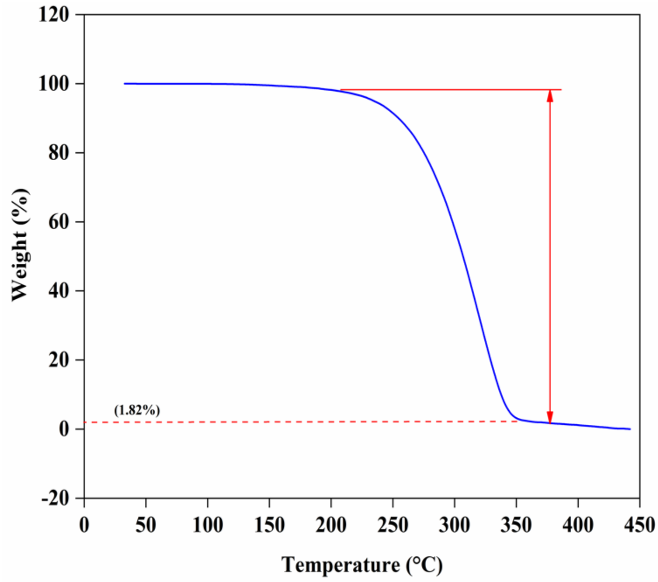

Fig. 1. Thermogravimetric analysis of paraffin (RT 58).

heating rate of 20 °C/min using an SDT Q600 analyzer. It can be seen from Fig.1, the degradation occurs after 216 °C with a reduced weight of 1.82 % [25]. Therefore, it is suited to the present study.

Table 1. Physical properties of circulating coolants

Properties	DI Water	Ethanol	Methyl acetate
Boiling point, T_s (°C)	99.2	78.3	57.1
Density, ρ_l (kg/m^3)	998.5	791	932
Dynamic viscosity, μ_l (Pa s)	0.00088	0.00113	0.00036
Heat of evaporation, L_v (kJ/kg)	2257	853	438
Surface tension, σ (N/m)	0.0728	0.0241	0.0239

Table 2. Properties of PCM

Properties	Paraffin wax
Density, ρ_s/ρ_l (kg/m^3)	890/760
Heat of fusion, L_f (kJ/kg)	241
Melting point, T_m (°C)	53
Specific heat capacity, $c_{p,s}/c_{p,l}$ (kJ/kg.K)	2.16/2.41
Thermal conductivity, k (W/m.K)	0.15

2.2. Description of test setup

Figure 2 depicts the schematic layout of a test setup for power harvesting in electronic modules. It has a fluid tank, primary PCM storage, conical manifold, cylindrical manifold, secondary PCM storage and non-return valve. A dimension of 0.1 × 0.1 × 0.1 m of the fluid tank is filled up with DI water, ethanol and methyl acetate respectively. The immersion coil heater (12 Ω, 400 W) is fixed inside the fluid tank and heat input to the setup varies from 60 to 110 W. A four copper tubes whose diameter of 0.0063 m is used to couple the fluid tank and conical manifold. The conical manifold is provided to promote the vapour flow rate. The primary PCM storage is used to store latent heat from the evaporative fluids whose diameter and length are 0.04 m and 0.15 m respectively. The fluid tank, conical manifold and primary PCM storage are made of stainless steel and insulated with 3 mm thickness of asbestos rope for avoiding the heat loss through convective heat transfer.

The cylindrical manifold is provided to enhance the condensation rate of circulating fluid. SBR tube is used between the cylindrical manifold and fluid tank to eliminate heat conduction. A non-return valve is imparted to avoid backflow of circulating fluid from the fluid tank. Thirteen T-type thermocouples (accuracy: ± 0.2 ˚C) are located at different positions and the temperature of various elements are measured by a data logger (Agilent 34970A, US). A U-tube manometer is provided to ensure the pressure drop between the entry and exit of primary PCM storage. It is measured to be negligible pressure drop during all experimentation.

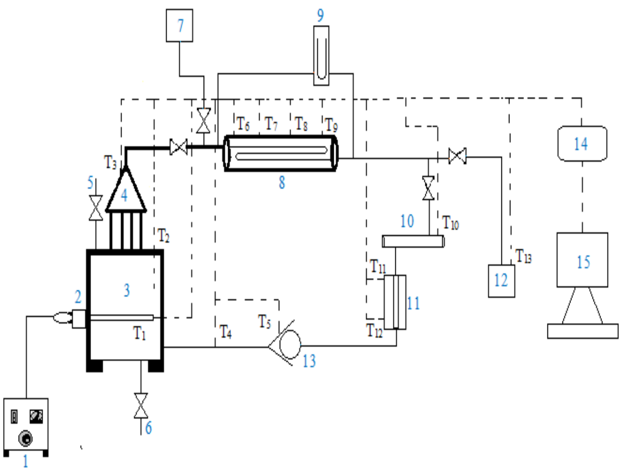

Fig. 2. Schematic layout of test setup for power harvesting in electronic modules

(1. Power supply 2. Heater 3. Fluid tank 4. Conical manifold 5. Fluid filling valve 6. Drainage valve 7. Cold water tank 8. Primary PCM storage 9. U-tube manometer 10. Cylinderical manifold 11. Secondary PCM storage 12. Hot water tank 13. Non-return valve 14. Data logger 15. Personal computer)

The working principle is based on evaporative cooling using thermosyphon aid PCM storage for power harvesting in a heat sink. During the heater is switched on, the liquid circulating fluid in the fluid tank gets heated up and converts it into vapour. Due to the low density, vapour rises to the upper surface of the conical manifold, thereby the flow rate is intensified. Then, the vapour is allowed to primary PCM storage through the inside copper pipe. Latent heat energy is exchanged between the vaporized fluid and PCM. It converts into condensed liquid and comes back into the fluid tank owing to the capillary effect. This process in a loop manner without the use of external aid. During the switched off condition, cold water is passed through the copper tube to primary PCM storage to solidify the molten PCM. The hot water outlet is collected for every one minute from the hot water tank.

2.3. Data reduction

The intensified thermal performance of the test setup is calculated as follows,

Rate of waste heat extraction by circulating fluid in percentage as

$$\left(Q_a / Q_l \right) \times 100 \tag{1}$$

where Q_a and Q_l are actual heat extracted and heat loss by convection respectively.

The actual heat extracted is estimated as

$$Q_a = Q_s - Q_l \tag{2}$$

The heat loss by convection is determined by

$$Q_l = h_{cv} A_{cv} [T_s - T_f] \tag{3}$$

where, $$h_{cv} = \frac{0.85(Gr\,\mathrm{Pr})^{0.188}.k}{D} \tag{4}$$

The thermal resistance is obtained as

$$R = \frac{(T_{ev} - T_{co})}{Q_s} \tag{5}$$

where Q_s, T_{ev} and T_{co} are the heat supply to the setup, evaporative temperature and condensation temperature respectively.

The vapour flow rate of circulating fluid,

$$\dot{m} = \frac{Q_s}{L_v} \tag{6}$$

where L_v is the heat of evaporation of circulating fluid.

The amount of heat energy stored by PCM is estimated as

$$Q_{st} = mc_{ps}[T_m - T_i] + mL_f + mc_{pl}[T_f - T_m] \tag{7}$$

where L_f is the heat of fusion of PCM; T_m, T_f and T_i are the melting, final and initial temperature of PCM respectively.

Power harvested by PCM,

$$P = \frac{Q_{st}}{t_{st}} \quad (8)$$

where t_{st} is the time at which the occurrence of the SST of PCM.

2.4. Uncertainty analysis

The maximum uncertainty in the heat input is calculated using eq. (10) [26]. The error of ammeter and voltmeter are 0.0020 Å and 0.0001 V.

$$\delta\sigma = \pm\sqrt{\sum_{i=1}^{N}\left(\frac{\partial\sigma}{\partial m_i}\times\delta m_i\right)^2} \quad (9)$$

For a maximum heat input (110 W) case,

$$\delta Q_s = \pm\sqrt{\left(\frac{\partial Q_s}{\partial V}\times\delta V\right)^2+\left(\frac{\partial Q_s}{\partial I}\times\delta I\right)^2} \quad (10)$$

$$\delta Q_s = \pm\sqrt{(I\times\delta V)^2+(V\times\delta I)^2} \quad (11)$$

$$\delta Q_s = \pm\sqrt{(1.1\times 0.0001)^2+(100\times 0.0020)^2}$$

$$\delta Q_s = \pm 0.2 \text{ W}$$

In terms of percentage, it can be expressed as $\frac{\delta Q_s}{Q_s}\times 100 = 0.18\%$

where V and I are voltage and current respectively.

3. Result and Discussion

The present study investigates the percentage of waste heat extraction and thermal resistance of the different circulating fluids. Also, the power harvested by PCM during charging and discharging is studied by the influence of vapourized DI water, ethanol and methyl acetate.

3.1. Percentage of waste heat extraction

Figure 3 depicts the percentage of waste heat extraction for circulating fluids with different heat inputs. It is seen that the increase of heat input is directly proportional to the percentage of waste heat extraction for all circulating fluids. At maximum heat input, DI water, ethanol and methyl acetate exhibit the waste heat extraction of about 96.5%, 97.7% and 98.7% respectively. It is because of the low heat of evaporation and boiling point of methyl acetate.

The vapour bubble formation is more for low heat of evaporation of circulating fluid at higher heat input. Also, the vapour flow rate increases by a low boiling point of circulating fluid. Nazari et al. [27] reviewed that the low boiling point is a deciding factor that induces the evaporation rate causes for the high heat transfer rate in low/medium temperature applications. The low heat of evaporation and boiling point of working fluid has a more activation in initial progress and hence the quantity of vapour enters into the condensation region will be more is reported by

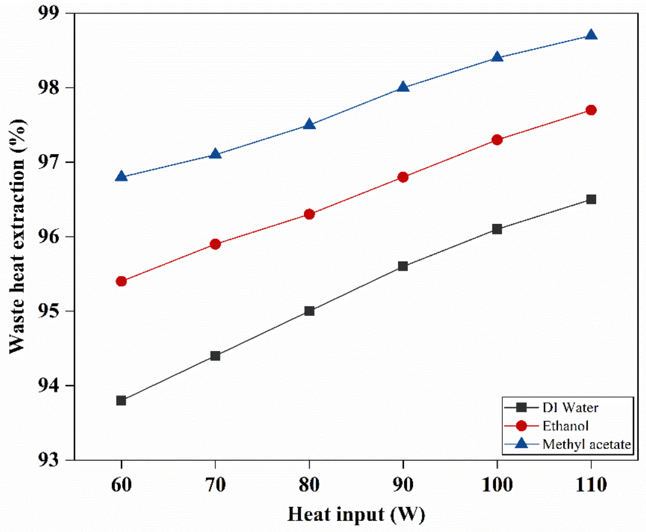

Fig. 3. Waste heat extraction by circulating coolants with different heat inputs

Naik et al. [28]. This is the reason that the percentage of waste heat extraction is high for methyl acetate in comparison with DI water and ethanol.

3.2. Thermal resistance

The thermal resistance is a crucial factor to obtain the intensified heat transfer rate. In general, the thermal resistance is inversely proportional to the heat input. Figure 4 shows the thermal resistance of DI water, ethanol and methyl acetate with heat inputs between 60 and 110 W. It is noticed that the low thermal resistance is obtained for methyl acetate at 110 W of about 0.237 K/W whereas 0.655 K/W and 0.398 K/W is found for DI water and ethanol respectively.

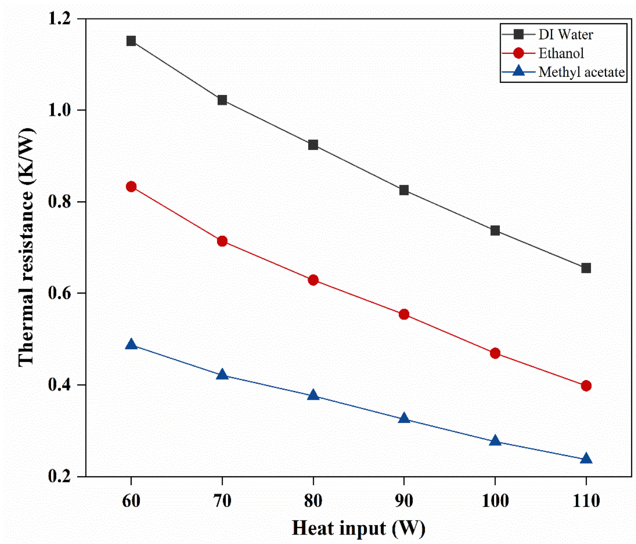

Fig. 4. Effect of heat input on thermal resistance for circulating coolants

At maximum heat input, the nucleate boiling starts to occur in the fluid tank that enhances the evaporation rate further causes more vapour flow rate to the condensation zone for low heat of evaporation circulating fluid. Table 3 represents the vapour flow rate of circulating fluids with different heat inputs. Naphon et al. [29] reported that superheat is more when increasing the heat load into maximum by natural convection. It is resulted that lower in thermal resistance in both condensation and evaporation section owing to high superheated mass flow rate. Also, the subcooling effect is reduced at high heat input. The velocity of circulating fluid is maximum when increasing the heat input from 60 to 110 W and hence the shear force is reduced between copper tube and the vapourized fluid which caused for lower in thermal resistance [30].

3.3. Power harvested by PCM during charging

The charging of PCM is analyzed until the primary stored PCM attains steady-state temperature (SST). The four T-type thermocouples have inserted in zigzag position with sequent order at primary PCM storage. The charging of PCM with the effect of vapourized circulating fluids with different flow rate is noted for the duration of every 5 min. Figure 5 depicts the temperature variation in PCM with different heat inputs between 60 and 110 W. As seen from Fig.5, the vapourized methyl acetate takes 90 min to reach SST of PCM at 110 W whereas DI water and ethanol take 145 min and 120 min aftermath remains constant till 200 min.

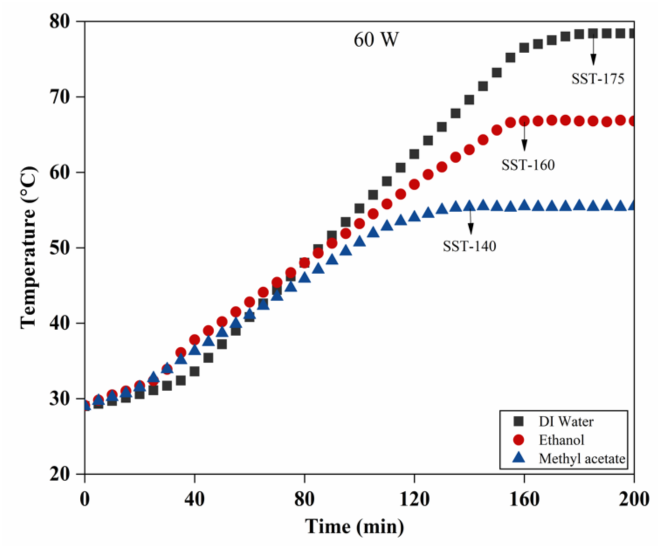

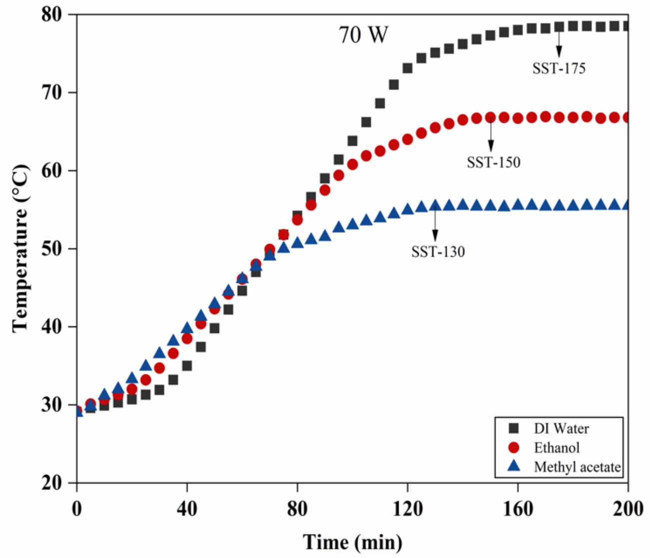

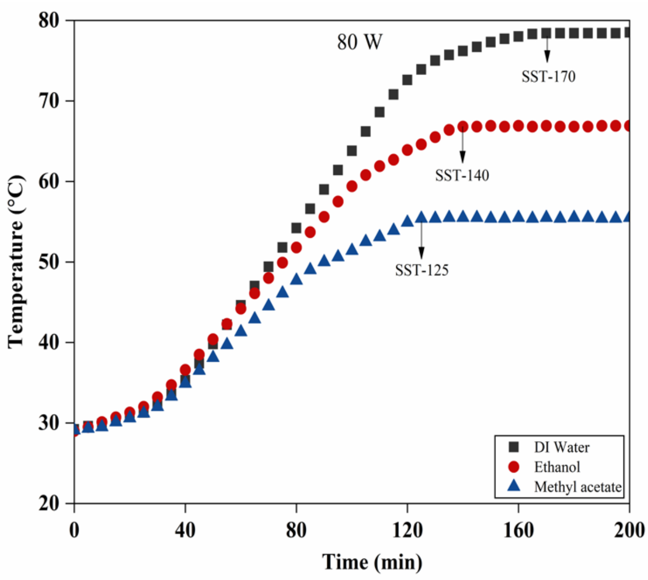

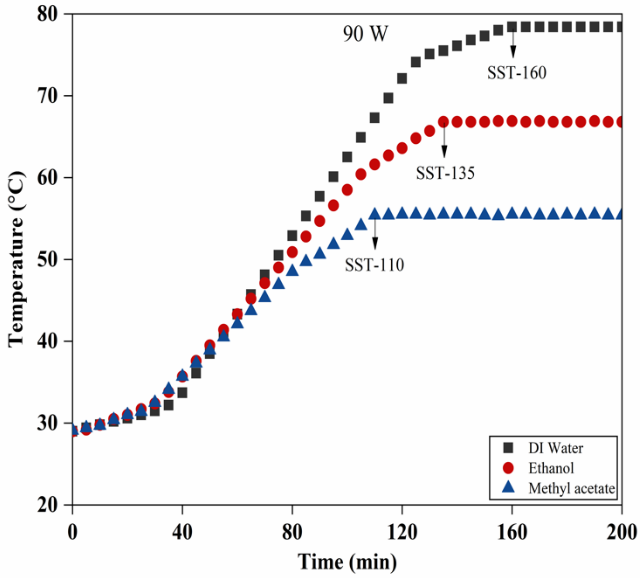

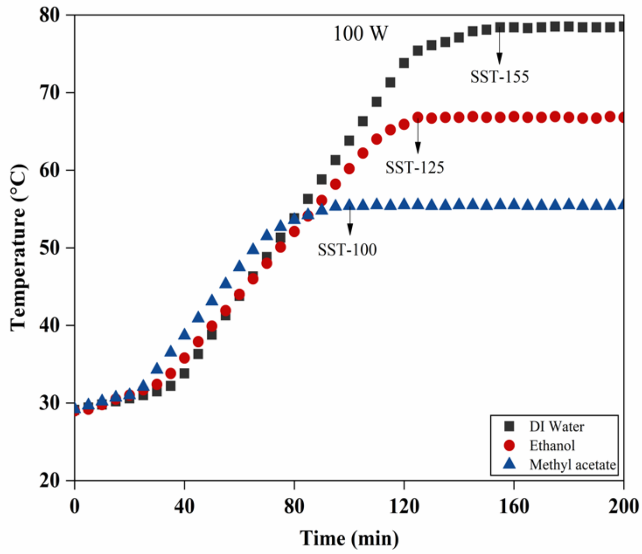

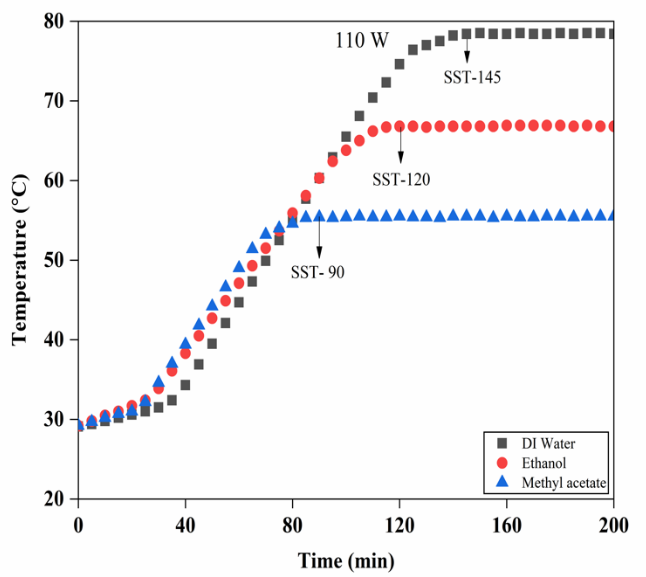

Fig. 5. Temperature variation in PCM during charging for heat input between 60 and 110 W

It is proposed that the charging of PCM depends on the vapour flow rate of circulating fluids. From the observations, it is noted that the PCM temperature is increased gradually until the first layer of PCM gets melted owing to conduction heat transfer between festoon copper tube and solid PCM [31]. Once the first layer converts into liquid PCM, then it changes as convection heat transfer which further causes faster in SST of PCM due to lower thermal resistance. It is seen from Fig.5, the heat input plays a vital role in charging the PCM. At 110 W, the vapour flow rate of circulating fluids is high thereby more heat is transferred into primary PCM storage resulting in lower time to achieves the SST of PCM. It is found that the vapour flow rate of DI water, ethanol and methyl acetate is 0.00292, 0.00774 and 0.01507 kg/min respectively at high heat input (Table 3). The PCM charging rate of vapourized methyl acetate and ethanol is 37.9% and 17.2% greater than DI water.

Table 3. Vapour flow rate of circulating coolants with different heat inputs

Heat input (W)	Vapour flow rate (kg/min)		
	DI Water	Ethanol	Methyl acetate
60	0.00160	0.00422	0.00822
70	0.00186	0.00492	0.00959
80	0.00213	0.00563	0.01096
90	0.00239	0.00633	0.01233
100	0.00266	0.00703	0.01370
110	0.00292	0.00774	0.01507

Table 4 presents the power harvested by PCM with the effects of vapourized circulating fluids for various heat inputs. It is observed that the power harvested by PCM is increased by the increase of heat input for all circulating fluids. The highest power harvested by PCM is obtained as 9.41 W for vapourized methyl acetate at 110 W due to high vapour flow rate and less time for attains SST of PCM.

Table 4. Power harvested by PCM with the effect of circulating coolants

Circulating coolants	Power harvested by PCM (W)					
	60 W	70 W	80 W	90 W	100 W	110 W
DI Water	5.42	5.73	5.90	6.27	6.47	6.92
Ethanol	5.77	6.16	6.60	6.84	7.39	7.70
Methyl acetate	6.04	6.51	6.77	7.69	8.46	9.41

Kalapala and Devanuri [32] reported that the increase of energy stored in PCM based on mass flow rate. Also, it is revealed that the increase in the mass flow rate of working fluid improves the heat transfer rate. Therefore, it is suggested that maximum power harvested by PCM shows a high percentage of waste heat extraction by circulating fluids in the intended electronic modules [33].

3.4. Discharging of PCM

The discharging of PCM is studied during the heater is switched off condition. The molten PCM is solidified by passing cold water through a festoon copper tube at a consistent flow rate. Then the latent heat is transferred to cold water from molten PCM and it gets outlet of hot water which is noted for every 1 min duration. Also, the temperature variation in PCM is noted and this process continued until PCM becomes solidified to its room temperature.

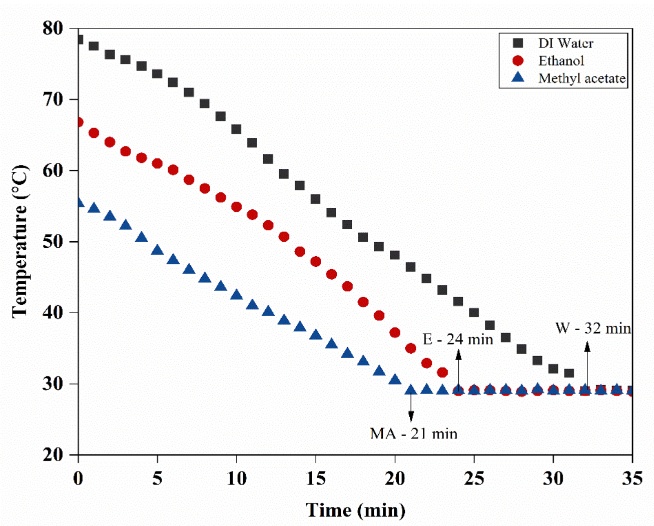

Fig. 6. Temperature variation in PCM during discharging for 110 W

Figure 6 shows the temperature variation in PCM during discharging at 110 W. As seen from Fig.6, the vapourized methyl acetate influenced molten PCM gets solidified from 55.4 to 29 °C in 21 min whereas DI water and ethanol influenced molten PCM to take 78.4 to 29 °C in 32 min and 66.8 to 29 °C in 24 min respectively. The time taken to solidify the PCM is noted for all heat inputs and is found to be same. At starting, the convection takes a part to solidify the molten PCM in faster during solidification. Aftermath, it converts into conduction heat transfer then the solidification becomes delayed [34]. Moreover, the heat transfer between supplied cold water and molten PCM is low due to the low thermal conductivity of PCM. It is noticed that the vapourized methyl acetate influenced molten PCM reaches room temperature quickly. It is mainly due to the discharging time is less for low SST of molten PCM.

4. Conclusion

A PCM based natural cooling (thermosyphon) is investigated for different circulating fluids to assess the power harvested in electronic modules. The experiments are conducted with different heat inputs between 60 and 110 W. The thermal performance and power harvested by PCM are studied simultaneously for DI water, ethanol and methyl acetate respectively. The waste heat extraction of 98.7% and low thermal resistance of about 0.237 K/W are obtained for methyl acetate at maximum heat input. It is because of the low heat of evaporation and less subcooling effect. During charging of PCM, the vapourized methyl acetate attains SST quickly by 90 min at 110 W whereas DI water and ethanol take 145 and 120 min. Also, the maximum power harvested by PCM is obtained as 9.41 W for vapourized methyl acetate at maximum heat input. This is because of high vapour flow rate and less time to reach SST of PCM. The methyl acetate influenced molten PCM takes quick solidification of about 21 min due to a low SST of molten PCM. It is suggested that the developed model is more efficient when methyl acetate as a circulating fluid in both switched on and off conditions. Hence, the created test setup is suitable for all desirable range of electronic modules that show saved sustainable energy using null electricity.

Acknowledgements

The authors are grateful to the Council of Scientific and Industrial Research (CSIR), New Delhi, Government of India for granting to this research work (ACK. No.: 141202/2K18/1).

Nomencluature

List of symbols

A	Area, m^2
c_{pl}	Specific heat of liquid, kJ/(kg.K)
c_{ps}	Specific heat of solid, kJ/(kg.K)
D	Diameter, m
Gr	Grashof number
h	Heat transfer coefficient, W/(m^2.K)
I	Current, A
k	Thermal conductivity, W/(m.K)
L_f	Heat of fusion, kJ/kg
L_v	Heat of evaporation, kJ/kg
m	Mass, kg
$\dot{m}$	Vapour flow rate, kg/min
P	Power harvested, W
Pr	Prandtl number
Q	Heat power, W
Q_a	Actual heat extracted, J
Q_l	Heat loss, J
Q_{st}	Stored heat energy, J
R	Thermal resistance, K/W
t	Time, min
T	Temperature, °C
T_f	Fluid temperature, °C
T_i	Initial temperature, °C
T_m	Melting temperature, °C
T_s	Surface temperature, °C
V	Voltage, V

Greek symbols

δ	Increment

Subscript

cv	Convection
co	Condensation
ev	Evaporation
s	Supplied
st	Steady state

References

[1] R. Ye, R. Huang, X. Fang, and Z. Zhang, "Simulative optimization on energy saving performance of phase change panels with different phase transition temperatures", Sustain. Cities Soc, Vol. 52, pp. 101833, Jan 2020.

[2] U.M. Choi, K.B. Lee, and F. Blaabjerg, "Power electronics for renewable energy systems: Wind turbine and photovoltaic systems", *International Conference on Renewable Energy Research and Applications (ICRERA)*, Nagasaki, pp. 1-8, Nov 2012.

[3] S. Duerr, C. Ababei, and D.M. Ionel, "Load balancing with energy storage systems based on co-simulation of multiple smart buildings and distribution networks", *IEEE 6th International Conference on*

Renewable Energy Research and Applications (ICRERA), San Diego, CA, pp. 175-180, Nov 2017.

[4] P. Visconti, J. Varona, R. Velázquez, N.I. Giannocaro, R. De Fazio, and M. Carrasco, "MEMS-based Micro-scale Wind Turbines as Energy Harvesters of the Convective Airflows in Microelectronic Circuits", *Int. J. Renew. Energy Res*, Vol. 10, No. 3, pp. 1213-1225, Sep 2020.

[5] S. Gareh, B.C. Kok, M.H. Yee, A.A. Borhana, and S. K. Alswed, "Development of a novel compression-based piezoelectric traffic model for improving the roadways energy harvesting system by applying the celular atomata traffic model", *Int. J. Renew. Energy Res*, Vol. 9, No. 4, pp. 2101-2111, Dec 2019.

[6] K. Kawabuchi, and T. Yachi, "Analysis of the heat transfer characteristics in a thermoelectric conversion device", *International Conference on Renewable Energy Research and Applications (ICRERA)*, Nagasaki, pp. 1-5, Nov 2012.

[7] N. Altin, "Energy storage systems and power system stability", *International Smart Grid Workshop and Certificate Program (ISGWCP)*, Istanbul, pp. 1-7, March 2016.

[8] F. Anggara, R.A. Anugrah, and H. Pranoto, "Thermal energy storage using horizontal shell-tube heat exchanger: numerical investigation on temperature variation of HTF", *Int. J. Renew. Energy Res*, Vol. 9, No. 4, pp. 2112-2117, Dec 2019.

[9] P. Kumar, S. Kumar, R. Kumar, and S. Mandal, "Numerical and experimental analysis of Scheffler concentrator receiver for steam generation using phase change material", *Int. J. Renew. Energy Res*, Vol. 8, No. 3, pp. 1339-1345, Sep 2018.

[10] T. Nehari, M. Benlekkam, D. Nehari, and A. Youcefi, "The effect of inclination on the passive cooling of the solar PV panel by using phase change material", *Int. J. Renew. Energy Res*, Vol. 6, No. 1, pp. 132-139, Mar 2016.

[11] R. Baby, and C. Balaji, "Thermal optimization of PCM based pin fin heat sinks: an experimental study", *Appl. Therm. Eng*, Vol. 54, No.1, pp. 65-77, May 2013.

[12] E.M. Alawadhi, and C. H. Amon, "PCM thermal control unit for portable electronic devices: experimental and numerical studies", *IEEE Trans. Components Packag. Technol*, Vol. 26, No. 1, pp. 116-125, Jun 2003.

[13] S.K. Sahoo, M.K. Das, and P. Rath, "Application of TCE-PCM based heat sinks for cooling of electronic components: A review", *Renew. Sustain. Energy Rev*, Vol. 59, pp. 550-582, Jun 2016.

[14] K.G. Kannan, R. Kamatchi, T. Venkatajalapathi, and A.S. Krishnan, "Enhanced heat transfer by thermosyphon method in electronic devices", *Inter. J. Heat Technol*, Vol. 36, No.1, pp. 339-343, Mar 2018.

[15] A. Goldoust, M.R.S. Emami, and A.A. Ranjbar, "Experimental investigation of the evaporator section tilted angle and filling ratio on the thermal characteristics of a two-phase closed thermosyphon", *Inter. J. Heat Technol*, Vol. 37, No. 2, pp. 569-574, Jun 2019.

[16] A. Samba, H. Louahlia-Gualous, S. Le Masson, and D. Norterhauser, "Two-phase thermosyphon loop for cooling outdoor telecommunication equipments", *Appl. Therm. Eng*, Vol. 50, No. 1, pp. 1351-1360, Jan 2013.

[17] Q. Liu, K. Fukuda, and P.F. Sutopo, "Experimental study on thermosyphon for ship board high-power electronics cooling system", *Heat Transf. Eng*, Vol. 35, No. 11-12, pp. 1077-1083, Jul 2014.

[18] M. Zhang, Z. Liu, and G. Ma, "The experimental investigation on thermal performance of a flat two-phase thermosiphon", *Int. J. Therm. Sci*, Vol. 47, No. 9, pp. 1195-1203, Sep 2008.

[19] A. Kamyar, K.S. Ong, and R. Saidur, "Effects of nanofluids on heat transfer characteristics of a two-phase closed thermosiphon", *Int. J. Heat Mass Transf*, Vol. 65, pp. 610-618, Oct 2013.

[20] M. Narcy, S. Lips, and V. Sartre, "Experimental investigation of a confined flat two-phase thermosyphon for electronics cooling", *Exp. Therm. Fluid Sci*, Vol. 96, pp. 516-529, Sep 2018.

[21] B. Palm, and R. Khodabandeh, "Choosing working fluid for two-phase thermosyphon systems for cooling of electronics", *J. Electron. Packag*, Vol. 125, No. 2, pp. 276-281, Jun 2003.

[22] J. Li, W. Tian, and L. Lv, "A thermosyphon heat pipe cooler for high power LEDs cooling", *Heat Mass Transf*, Vol. 52, No. 8, pp. 1541-1548, Aug 2016.

[23] J. Krishna, P.S. Kishore, and A.B. Solomon, "Heat pipe with nano enhanced-PCM for electronic cooling application", *Exp. Therm. Fluid Sci*, Vol. 81, pp. 84-92, Feb 2017.

[24] M.T. Chaichan, and H.A Kazem, "Using aluminium powder with PCM (paraffin wax) to enhance single slope solar water distillation productivity in Baghdad–Iraq winter weathers", *Int. J. Renew. Energy Res*, Vol. 5, No. 1, pp. 251-257, Mar 2015.

[25] M. Gonen, D. Balkose, F. Inal, and S. Ulku, "The effect of zinc stearate on thermal degradation of paraffin wax", *J. Therm. Anal. Calorim*, Vol. 94, No. 3, pp. 737-742, Dec 2008.

[26] S. P. Venkateshan, *Mechanical Measurements*, New Delhi, India: Ane Books, 2008.

[27] M.A. Nazari, M. H. Ahmadi, R. Ghasempour, and M. B. Shafii, "How to improve the thermal performance of pulsating heat pipes: A review on working fluid", *Renew. Sustain. Energy Rev*, Vol. 91, pp. 630-638, Aug 2018.

[28]R. Naik, V. Varadarajan, G. Pundarika, and K.R. Narasimha, "Experimental investigation and performance evaluation of a closed loop pulsating heat pipe", *J. Appl. Fluid Mech*, Vol. 6, pp. 267-275, Jan. 2013.

[29]P. Naphon, S. Wiriyasart, and S. Wongwises, "Thermal cooling enhancement techniques for electronic components", *Int. Commun. Heat Mass Transf*, Vol. 61, pp. 140-145, Feb 2015.

[30]K.G. Kannan, and R. Kamatchi, "Augmented heat transfer by hybrid thermosyphon assisted thermal energy storage system for electronic cooling", *J. Energy Storage*, Vol. 27, pp. 101146, Feb 2020.

[31]L.N. Narasimhan, "Assessment of latent heat thermal storage systems operating with multiple phase change materials", *J. Energy Storage*, Vol. 23, pp. 442-455, Jun 2019.

[32]L. Kalapala, and J.K. Devanuri, "Influence of operational and design parameters on the performance of a PCM based heat exchanger for thermal energy storage–A review", *J. Energy Storage*, Vol. 20, pp. 497-519, Dec 2018.

[33]S. Kotra, and M.K. Mishra, "Energy management of hybrid microgrid with hybrid energy storage system", *International Conference on Renewable Energy Research and Applications (ICRERA)*, Palermo, pp. 856-860, Nov 2015.

[34]Y.H. Diao, S. Wang, C.Z. Li, Y.H. Zhao, and T.T. Zhu, "Experimental study on the heat transfer characteristics of a new type flat micro heat pipe heat exchanger with latent heat thermal energy storage", *Exp. Heat Transf*, Vol. 30, No. 2, pp. 91-111, Mar 2017.